Field enhancement in single subwavelength apertures

Evgeny Popov, Michel Nevière, Jérôme Wenger, Pierre-François Lenne, Hervé Rigneault, and Patric Chaumet

Institut Fresnel, Domaine Universitaire de Saint Jérôme, Université d'Aix Marseille III, CNRS UMR 6133, 13397 Marseille Cedex 20, France

Nicolas Bonod

Commissariat à l'Énergie Atomique, Centre d'Études Scientifiques et Techniques d'Aquitaine, BP2, 33114 Le Barp, France

José Dintinger and Thomas Ebbesen

Institut des Sciences et Ingénière Supramoléculaires, Université Louis Pasteur, CNRS UMR 7006, 8 Allée G. Monge, 67000 Strasbourg, France

Received December 2, 2005; revised March 7, 2006; accepted March 9, 2006; posted March 16, 2006 (Doc. ID 66426)

A peak of the detected fluorescence rate per molecule has recently been observed in experiments of fluorescence correlation spectroscopy carried out on subwavelength apertures in metallic screens, a phenomenon that appears at a diameter-to-wavelength ratio below the fundamental mode cutoff. Although the origin of the resonant transmission through a subwavelength aperture has been well explained in terms of excitation of plasmon surface modes on the aperture ridge, the origin of the maximum that occurs at a radius-to-wavelength ratio smaller than 1/4 was not clear. Using a rigorous electromagnetic theory of light diffraction in cylindrical geometry, we show that it is linked to the appearance of the fundamental mode propagating inside the aperture. We obtain good agreement between the theoretical and the experimental results. © 2006 Optical Society of America

OCIS codes: 300.2530, 050.1220, 050.1940.

1. INTRODUCTION

Since the experimental breakthrough by Ebbesen and co-workers[1,2] on the extraordinary transmission of light through periodic and single holes milled in a metallic screen, several new fields of research have emerged, taking advantage of the amazing properties of these nanostructures. While the array periodicity can excite resonantly surface plasmons,[3–6] light diffraction on single holes has been shown to lead to many interesting physical phenomena, such as the excitation of local surface plasmon modes,[2,7] the edge effects due to current discontinuities,[8,9] and the excitation of evanescent or propagation modes of the hollow circular waveguide formed inside the aperture.[10,11]

The ability to localize light in spots much smaller than the volume predicted by diffraction theory offers attractive applications in biophotonics, such as probing a few molecules in a highly concentrated solution[12–14] or monitoring a cell membrane with a submicrometer resolution.[15,16] A second property is the ability to enhance the fluorescence signal emitted within the nanoapertures. While this effect was first experimentally proven for periodic or random arrays of nanoapertures,[17–20] recent work has independently demonstrated that a single subwavelength aperture could also lead to a significant enhancement of the fluorescence rate emitted per molecule,[13,21] when the diameter-to-wavelength ratio is smaller than 1/4, just below the cutoff of the fundamental mode that can propagate inside the hole.

The aim of this paper is to numerically investigate the excitation field enhancement for a circular subwavelength aperture milled in a real aluminum film, to compare the results with the experiment, and to provide a physical explanation for this phenomenon.

2. FIELD ENHANCEMENT INSIDE SINGLE SUBWAVELENGTH APERTURES AND THE ROLE OF LOSSES

Figure 1 presents a cross section of the geometry under study. It consists of a 220 nm thick aluminum layer deposited on a glass slice and pierced by single holes having different diameters and illuminated from the plate side by a normally incident plane wave linearly polarized in the x direction. The aperture and the substrate region are filled with liquid, which is the solvent used in the fluorescence experiment described below. While most of the research on transmission through subwavelength holes use silver or gold screens, the choice of aluminum already made in Ref. 13 is due to the tarring of silver in air and to the drop of gold reflectivity below 550 nm.

Figures 2(a) and 2(b) present numerical and experimental results on the electric field intensity as a function of the aperture radius for two different wavelength val-

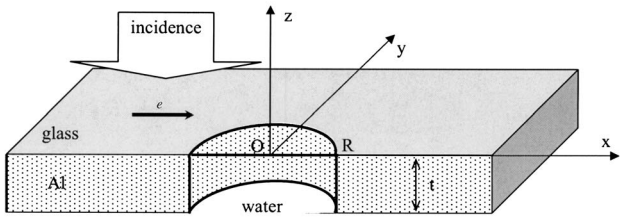

Fig. 1. Schematic representation of a circular aperture in a metallic film and notations.

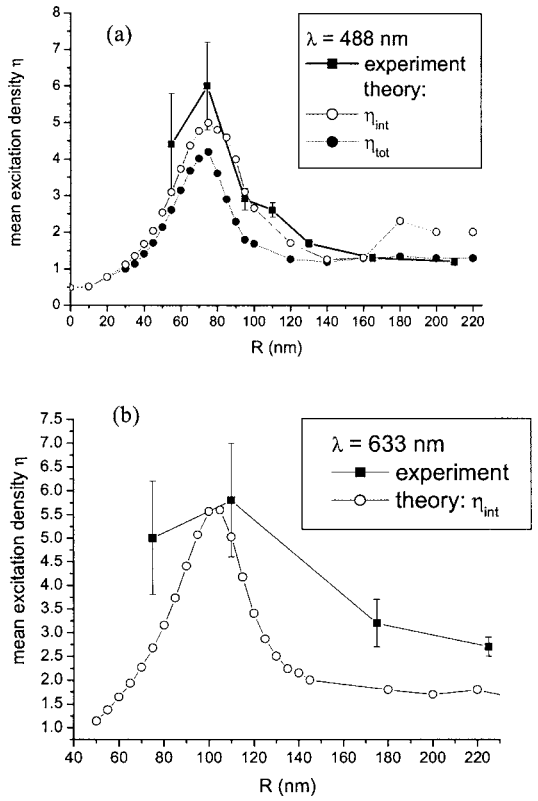

Fig. 2. Mean excitation density η of the electric field as a function of the radius of a circular aperture in an aluminum film with thickness of 220 nm; the cladding is glass, and the substrate and aperture material are water. Open circles, excitation density taken inside the aperture; solid circles, the integration volume consisting of the region inside the aperture plus a cylinder with 10 μm diameter and 3 μm height after the aperture. Squares, experimental enhancement of the fluorescence rate per molecule. (a) Wavelength equal to 488 nm, with Rhodamine 6G as the fluorescent reporter. (b) Wavelength of 633 nm with Cyanine 5 as a fluorescent dye.

ues. The experiment at an excitation wavelength of 488 nm is made with Rhodamine 6G (which reemits at 550 nm), while at 633 nm the fluorescent molecule was Cyanine 5, which reemits at 650 nm. The experimental results correspond to the ratio between the measured fluorescence rate per molecule inside the aperture and the fluorescence rate per molecule in an open solution (the incoming excitation power is fixed and carefully set to avoid photobleaching and saturation of the fluorescence emission; more details on the experimental apparatus and data analysis are given in Ref. 13).

The numerical results are obtained using the differential method in cylindrical coordinates described in Ref. 22. Unfortunately, the recent state of the theoretical method does not allow modeling of the emission by a dipole inside the aperture, so the calculations concern only the excitation field. The refractive indices are equal, respectively, to $n_{\mathrm{glass}}=1.5$ for the substrate, $n_w=1.4$ for the solvent, $n_{\mathrm{Al}}=0.6276+i5.4524$ at 488 nm, and $n_{\mathrm{Al}}=1.2126+i6.9258$ at 633 nm for the metallic layer. The mean excitation density η (over the probed nanoaperture volume) is defined as the total excitation intensity I_V per unity of effective volume V_{eff}:

$$\eta = I_V / V_{\mathrm{eff}}, \tag{1}$$

where the excitation intensity is given by

$$I_V = \int_V |E|^2 \mathrm{d}V. \tag{2}$$

We focus here on the role played by the excitation field on the observed fluorescence enhancement, and therefore we make the assumption that the local collection efficiency is uniform and set to unity over the entire observation volume. In this case, the effective volume is defined as usual in confocal fluorescence microscopy[23]:

$$V_{\mathrm{eff}} \equiv \frac{\left(\int_V |E|^2 \mathrm{d}V\right)^2}{\int_V |E|^4 \mathrm{d}V}. \tag{3}$$

The numerical integration of the field intensity is made over two different volumes V of integration. The first one V_{int} consists of the region inside the aperture and provides the values η_{int} presented with open circles in Fig. 2. The second volume V_{tot} contains the inner part of the aperture plus a region below the screen extended in a cylinder with 10 μm diameter and 3 μm height. Outside this volume the electric field intensity drops to 1/1000 of its value on the aperture exit. The mean excitation density calculated inside this volume is called η_{tot} and is denoted by solid circles. Its values are slightly lower than the mean excitation density η_{int} inside the aperture. The difference is negligible for small apertures, as long as the electric field penetration below the screen is quite weak (intensity of the order of 10^{-13} without a hole). The difference between the two densities increases with the hole radius, as the transmission due to the aperture is growing on and becomes significant above the fundamental cutoff (see Fig. 3).

The theoretical results follow well the experimental data, indicating that almost the entire enhancement of the fluorescence rate per molecule can be explained by the increase of the mean excitation density. However, there is a systematic difference between the experimental data and the theoretical model. This effect is possibly due to the influence of the aperture on the local collection efficiency, which is obviously not constant over the whole nanoaperture volume and needs to be taken into account to fully model the experimental observations. Note that the local collection efficiency stands for the electromagnetic power emitted by a dipole located inside the aperture, which is collected by the detector. In this respect, it

includes the radiation pattern alteration and the possible lifetime reduction. The complete description of the fluorescence enhancement process would require the calculation of the local collection efficiency. However, this is beyond the scope of this paper.

Since the field intensity strongly varies within the hole depth (see Fig. 3), we shall compare its values calculated at a fixed distance (i.e., fixed value of z) from the aperture entrance on the metal–glass interface. The mean field intensity I_S is defined as the integral per unit surface over the aperture cross section S:

$$I_S = \frac{1}{\pi R^2} \int_S |\mathbf{E}| \mathrm{d}\boldsymbol{S}. \tag{4}$$

One can note in Fig. 2 that at low aperture radius the increase of the aperture surface leads to an increase of the mean excitation density η. This is due to several different effects and could be predicted from the perturbation analysis.[24] First, the aperture acts as a defect that diffracts the incident light. This effect originates from the aperture and is thus strongly localized inside the hole and is rapidly decreasing in all directions. Second, as described in Section 1, edge effects lead to an accumulation of charges on the edges, which additionally enhances the local field. The third effect is the excitation of local surface plasmons propagating away from the aperture along the metallic–dielectric interfaces. Due to the linear polarization of the incident light, all these effects are highly anisotropic,[8,24] but one can observe a clear tendency in the behavior of the mean excitation; it increases with R until reaching a maximum at a value of R approximately equal to 1/4.5 of the wavelength inside the solvent for the two excitation wavelengths used experimentally (for example, λ/n_w is equal to 348.5 nm while the optimal radius R_m is equal to 75 nm at a wavelength of 488 nm). Of course, one can always expect the existence of one or several maxima in the curves. For instance, for sufficiently large radii, the field is dominated by the Fresnel transmission through the glass–solvent interface, yielding a mean intensity I_S equal to 1.07 times the incident field intensity, at least in the limit when $R \to \infty$. The amazing fact is that the maximum occurs at such small aperture dimensions, much smaller than the dimensions that are the optimal ones for plasmon excitation on the glass–aluminum interface,[24] an effect known to be responsible for the extraordinary transmission through subwavelength holes. It turns out that the maximum of the mean excitation field (and of the fluorescence that it causes) occurs just below the cutoff of the fundamental mode that can propagate inside the hole. We will show that the appearance of a propagating mode increases absorption losses, which thwart the increase of the mean excitation field, and forms a maximum just below the cutoff.

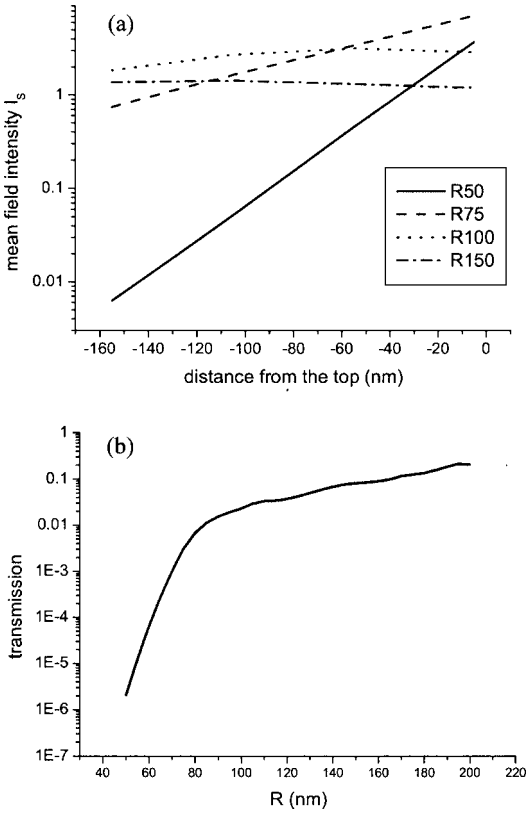

Fig. 3. (a) Mean field intensity I_S inside the aperture as a function of the depth for four different radii and fixed layer thickness ($t = 220$ nm). Parameters are as in Fig. 2(a). (b) Transmission defined as the ratio between the transmitted and the incident energy flux as a function of the radius. Parameters are as in Fig. 2(a). The flux is measured through a circle of radius equal to the wavelength and positioned after the aperture for the transmission and before the aperture for the incident wave.

Figure 3(a) shows the decrease of the mean field intensity I_S inside the hole depth (for a fixed metallic layer thickness equal to 220 nm) for several different aperture radii. The behavior of the field inside the hole (at least for narrow holes) is determined mainly by the fundamental waveguide mode, evanescent or propagating inside the hollow metallic waveguide representing the hole. It is well known that this mode has a cutoff below which the light field cannot propagate and rapidly decreases inside the hole depth. The smaller the radius, the faster the decrease, as observed in Fig. 3(a). Above the cutoff radius, the mode is propagating and is only slightly decreasing due to ohmic losses on the hole walls. This is why when looking at transmission properties of the aperture [Fig. 3(b)], the field enhancement at smaller radii cannot be observed if the layer thickness is sufficient to attenuate the field at the hole exit. However, if the screen is thin enough (for example, $t < 50$ nm), Fig. 3(a) would predict that the transmission should be higher for $R = 75$ nm (below the cutoff) than for $R = 100$ nm (above the cutoff).

For metals with infinite conductivity, the cutoff radius (or wavelength) is given by the zero of the corresponding Bessel function or its derivative.[25] For real metals, the cutoff radius is slightly smaller due to the fact that light penetrates inside the metal. In addition, due to the refractive index dispersion, the deviation from the infinitely conducting metal is wavelength dependent. Figure 4 enables us to compare the enhancement of the mean field intensity I_S calculated at the aperture entrance ($z = -5$ nm) as a function of the hole radius [Fig. 4(a)] and the real and imaginary parts of the fundamental mode normalized propagation constant γ [Fig. 4(b)], defined as the ratio between the mode propagation constant in the z direction and the free-space wavenumber:

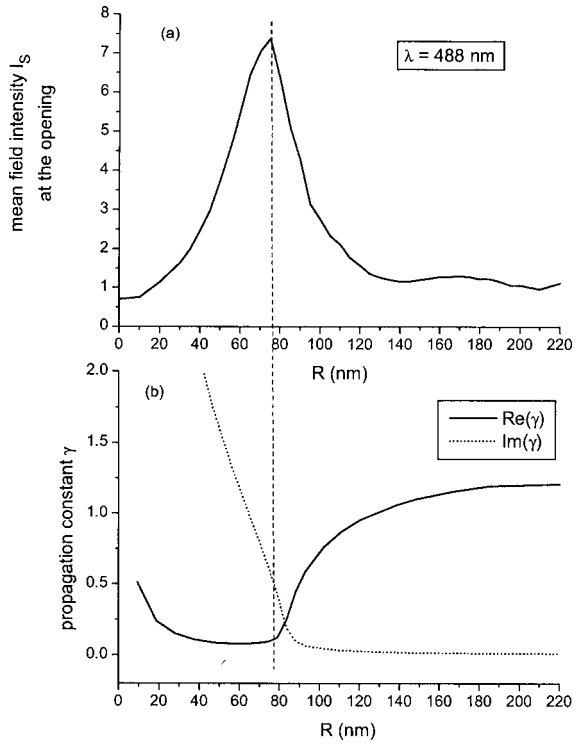

Fig. 4. (a) Mean electric field intensity I_S at a depth of $z=-5$ nm inside the aperture as a function of aperture radius. Wavelength is equal to 488 nm, aluminum layer thickness is 220 nm, the cladding is glass, and the solvent refractive index is 1.4. (b) Real and imaginary parts of the mode normalized propagation constant inside the hollow metallic waveguide inside the aperture.

$$\gamma = k_z/k_0. \tag{5}$$

It becomes evident that the drop in the mean intensity [and thus of the mean excitation density, Fig. 2(a)] starts in the region below the cutoff, although for a lossy waveguide the cutoff is not accurately defined. We can assume that it appears where the real and imaginary parts of the propagation constant become almost equal, because at that point the derivative of the propagation constant has a maximum, corresponding to a minimum of the group velocity. As is well known, in this region the absorption losses of the mode increase significantly, which leads to a drop in local field intensity. This behavior is typical of all resonant phenomena in lossy media, which increases the absorption (see Section 3 for clear evidence in the case of classical lamellar gratings). However, one can wonder why I_S continues decreasing for larger radii, although the imaginary part of the mode propagation constant becomes insignificant. One possible explanation can be found in the theory of photonic crystals. The maximum density of the states (in our case, the waveguide modes) appears exactly at the boundaries of the forbidden zone (i.e., at the cutoff) and decreases inside the allowed propagation zone (i.e., above the cutoff); thus the mode excitation strength decreases above the cutoff. Phrased differently, this means that when the group velocity (inversely proportional to the derivative of the propagation constant) is minimal, the mode excitation is maximal. Since above the cutoff the group velocity increases, there is no increase of I_S above the cutoff. Thus, at one side, the maximum of the electric field intensity is expected to appear exactly at the cutoff,[26] as happens in the case of a rectangular aperture pierced in a perfectly conducting screen.[27] However, the absorption losses are also maximal at this point[28] (as is clearly visible in Fig. 8 below), so that the maximum of I_S is slightly shifted from the cutoff position.

The same conclusion can be drawn at the other excitation wavelength of 633 nm. Figures 5(a) and 5(b) present the variation as a function of the hole radius of the mean field intensity and of the real and the imaginary part of the fundamental mode propagation constant, respectively. As already viewed in Fig. 2(b), here again we observe an increase in the mean field for small radii and a drop in the region where the fundamental mode becomes propagating. As in the case given in Fig. 4, the maximum enhancement takes place when the aperture radius is ~1/4.5 of the optical wavelength inside the aperture ($\lambda/n_w = 452.1$ nm and the optimal radius is $R_m = 103$ nm). Of course, due to the dependence of the cutoff on metal permittivity, the ratio between the optimal aperture radius and the wavelength will be different for other metals and will somehow depend on the wavelength.

To confirm the link between the drop in the mean excitation density (and intensity) and the position of the mode cutoff, we made a numerical experiment to separate this condition from the condition of optimal plasmon excitation on the metallic surface. This optimal condition is described in detail in Ref. 24, and for a glass–aluminum interface it lies close to hole radius values equal to 120 nm. To move the fundamental mode cutoff away from this value of R, we have doubled the refractive index of the filling medium ($n_w = 2.8$). The theoretical curve (Fig. 6)

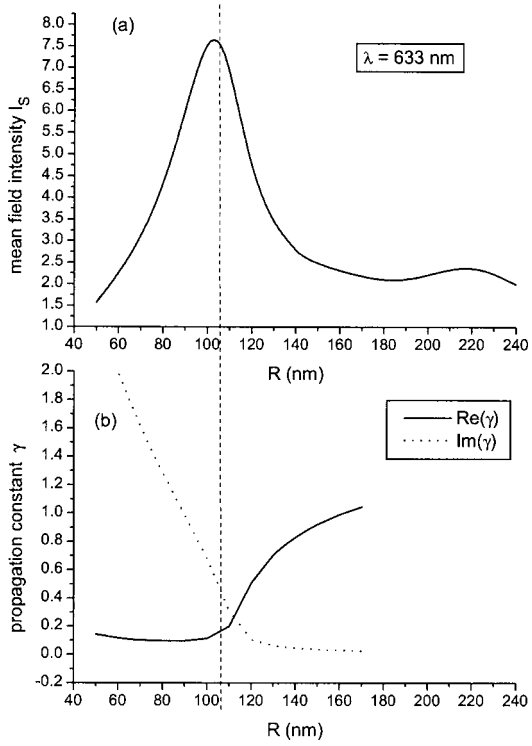

Fig. 5. As in Figs. 4(a) and 4(b) but for a wavelength equal to 633 nm.

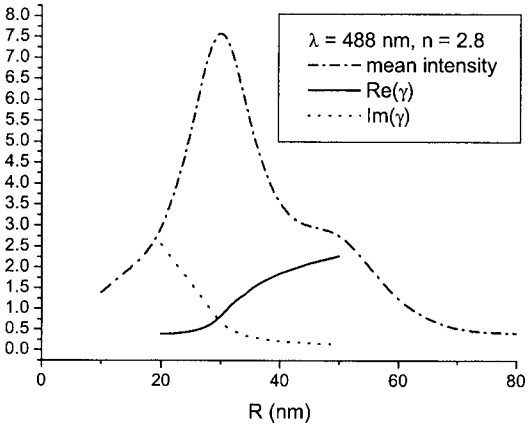

Fig. 6. As in Fig. 4 but for a different refractive index of the material inside the aperture equal to 2.8.

shows the same behavior of the mean field intensity: an enhancement for small radii and a decrease starting just below the fundamental mode cutoff. Due to the higher index of the filling material, this happens for smaller values of R, well separated from the optimal conditions of surface plasmon excitation, presenting proof that the peak is not linked to the excitation of a plasmon along the metallic surface.

3. RESONANT ABSORPTION IN METALLIC GRATINGS

To confirm the explanation of the origin of the peak in the mean field intensity inside the aperture (and thus of the maximum of fluorescence), in this section we study a one-dimensional model in which no surface plasmon can be excited. This is the case of a metallic grating with lamellar grooves illuminated in TE polarization, with the electric field vector parallel to the grooves.

Resonant field enhancement and absorption in metallic gratings have been a topic of extensive study for more than a century, starting with the famous work of R. Wood.[29] It is beyond the scope of this paper to review this area; an interested reader can look at Refs. 30–32. It is worth mentioning that the resonant plasmon excitation can lead to a total absorption of incident light (Brewster's effect in metallic gratings[33]) and absorption due to cavity resonances in lamellar gratings.[34]

Here we present a numerical study of the absorption, due to a guided mode excitation inside the grooves of a lamellar metallic grating with a metallic substrate. This appears to be closely related to the anomalous field enhancement and its decrease, discussed in Section 2. Figure 7 presents the dependence of the total reflected energy by a lamellar aluminum grating in a geometry similar to Fig. 1. The cladding is glass, the grooves are filled with the same solvent, and the substrate and the lamellae are metallic. The period is equal to 3 μm, large enough to prevent direct field coupling due to tunneling through the lamellae walls. The wavelength is equal to 488 nm at normal incidence in TE polarization (electric field vector parallel to the groove direction), chosen to avoid the existence of the fundamental TEM mode in TM polarization, which has no cutoff. Two different values of the groove depth are chosen to distinguish the effect in shallow and deep gratings. There are several propagating diffraction orders and the sum of their efficiencies is presented in Fig. 7 as a function of the groove width. Several anomalies are observed, consisting of enhanced absorption at some specific groove widths. The shallow grating is characterized by dips in the total reflectivity, i.e., peaks in absorption (which is complementary to unity to the reflectivity). When the grating is very deep, each dip increases the total absorption without recovering the reflectivity as the groove width is increased further on, contrary to what happens with the shallow grating.

To identify the phenomenon, Fig. 8(a) presents a zoom of Fig. 7 for small values of the groove width. As for a circular aperture, the modes in TE polarization inside the hollow waveguide formed by the groove walls bear a cutoff waveguide thickness. This is shown in Fig. 8(a) for the fundamental mode in which the propagation constant passes from almost imaginary to almost real value. By "almost" we mean that it is responsible for the peak (shallow grating) or the staircaselike (for deep grooves) increase in absorption. Absorption peaks for the shallow grating appear exactly with the appearance of the mode (cavity resonance). The fact that this mode becomes propagating increases its penetration inside the groove depth, together with the absorption as it propagates with losses (its propagation constant is then almost real, but not completely). In the same way as it happens for circular apertures, the mean field intensity, calculated at the groove opening, increases at first with the groove width [Fig. 8(b)], exhibits a maximum value just before the mode becomes propagating, and then decreases again. The enhancement of the mean field is less pronounced than for circular apertures because in TE polarization there is no plasmon excitation along the metallic surface and there are no edge effects (accumulation of charges at the edges) as long as the electric field is continuous everywhere. However, a peak similar to the peaks in discussed in Section 2 is observed.

The other anomalies in Fig. 7 can be identified with the appearance of higher-order waveguide modes inside the grooves as their width increases.

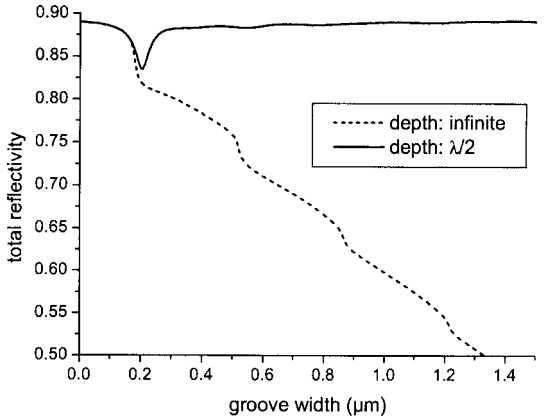

Fig. 7. Total energy reflected in all propagating diffraction orders as a function of the groove width for an aluminum lamellar grating with period equal to 3 μm. Wavelength is equal to 488 nm in TE polarization, cladding is glass, and filling material has a refractive index equal to 1.4. Two different groove depths, 0.25 μm and infinitely deep grooves.

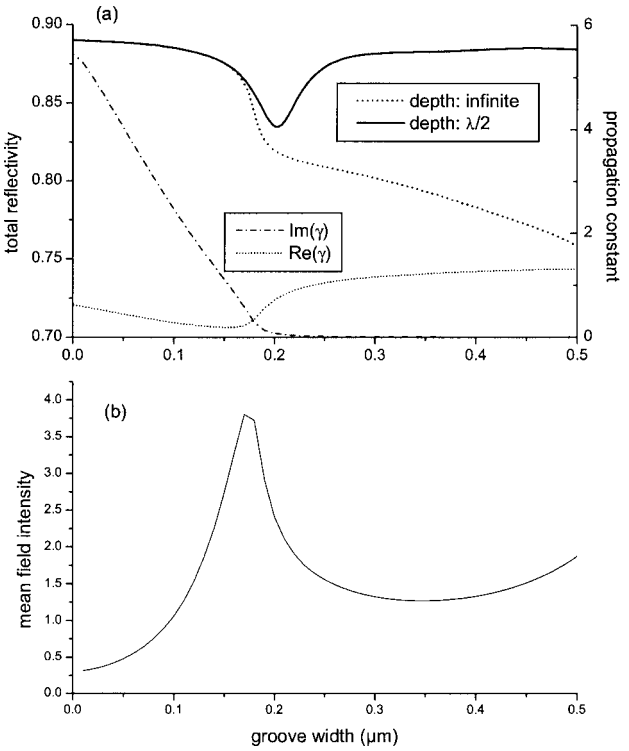

Fig. 8. (a) Closeup of Fig. 7, together with the groove width dependence of the normalized propagation constant of the fundamental mode, evanescent or propagating inside the plane hollow metallic waveguide formed by the groove walls. (b) Mean electric field intensity at the groove opening as a function of the groove width.

4. CONCLUSION

Using a rigorous electromagnetic analysis, we have demonstrated that the experimentally observed enhancement of the fluorescence in subwavelength single holes can be essentially explained by the variation of the mean excitation field intensity at the excitation wavelength. By modeling the diffraction of light by a single hole pierced in a metallic screen and by a lamellar metallic grating, we have shown that the appearance of the fundamental propagating mode of the hollow metallic waveguide inside the hole or the grating grooves leads to a sharp increase of the absorption losses, which accounts for the drop of the mean field intensity inside the aperture.

The fact that a significant increase in the fluorescence is obtained for small-radius apertures can be especially interesting because it allows for the possibility to significantly reduce the excitation while still detecting a sufficient signal. This yields an efficient signal-to-background discrimination, even with attoliter volume and single-molecule resolution.[13] The remaining systematic mismatch between the theoretical results and the experimental data could be due to the influence of the aperture on the emission properties of the fluorescent molecules, a phenomenon that requires further investigation.

ACKNOWLEDGMENTS

This work is supported by the French Ministry of Research (ACI Nanosciences).

Corresponding author E. Popov can be reached at e.popov@fresnel.fr.

REFERENCES

1. T. W. Ebbesen, H. J. Lezec, H. F. Ghaemi, T. Thio, and P. A. Wolff, "Extraordinary optical transmission through subwavelength hole arrays," Nature **391**, 667–669 (1998).
2. H. J. Lezec, A. Degiron, E. Devaux, R. A. Linke, L. Martin-Moreno, F. J. Garcia-Vidal, and T. W. Ebbesen, "Beaming light from a subwavelength aperture," Science **297**, 820–822 (2002).
3. H. F. Ghaemi, T. Thio, D. E. Grupp, T. W. Ebbesen, and H. J. Lezec, "Surface plasmons enhance optical transmission through sub-wavelength holes," Phys. Rev. B **58**, 6779–6782 (1998).
4. L. Martin-Moreno, F. J. Garcia-Vidal, H. J. Lezec, K. M. Pellerin, T. Thio, J. B. Pendry, and T. W. Ebbesen, "Theory of extraordinary optical transmission through subwavelength hole arrays," Phys. Rev. Lett. **86**, 1114–1117 (2001).
5. L. Salomon, F. Grillot, A. Zayats, and F. de Fornel, "Near-field distribution of optical transmission of periodic subwavelength holes in a metal film," Phys. Rev. Lett. **86**, 1110–1113 (2001).
6. A. Krishnan, T. Thio, T. J. Kima, H. J. Lezec, T. W. Ebbesen, P. A. Wolf, J. Pendry, L. Martin-Moreno, and F. J. Garcia-Vidal, "Evanescently-coupled surface resonance in surface plasmon enhanced transmission," Opt. Commun. **200**, 1–7 (2001).
7. A. Degiron, H. J. Lezec, N. Yamamoto, and T. W. Ebbesen, "Optical transmission properties of a single subwavelength aperture in a real metal," Opt. Commun. **239**, 61–66 (2004).
8. R. Zakharian, M. Mansuripur, and J. V. Moloney, "Transmission of light through small elliptical apertures," Opt. Express **12**, 2631–2648 (2004).
9. E. Popov, N. Bonod, M. Nevière, H. Rigneault, P. F. Lenne, and P. Chaumet, "Surface plasmon excitation on a single subwavelength hole in a metallic sheet," Appl. Opt. **44**, 2332–2337 (2005).
10. E. Popov, M. Nevière, P. Boyer, and N. Bonod, "Transmission through single apertures," Opt. Commun. **255**, 338–348 (2005).
11. R. Gordon and A. Brolo, "Increased cut-off wavelength for a subwavelength hole in a real metal," Opt. Express **13**, 1933–1938 (2005).
12. M. J. Levene, J. Korlach, S. W. Turner, M. Foquet, H. G. Craighead, and W. W. Webb, "Zero-mode waveguides for single-molecule analysis at high concentrations," Science **299**, 682–686 (2003).
13. H. Rigneault, J. Capoulade, J. Dintinger, J. Wenger, N. Bonod, E. Popov, T. W. Ebbesen, and P. F. Lenne, "Enhancement of single molecule fluorescence detection in subwavelength apertures," Phys. Rev. Lett. **95**, 117401 (2005).
14. K. T. Samiee, M. Foquet, L. Guo, E. C. Cox, and H. G. Craighead, "Lambda repressor oligomerization kinetics at high concentrations using fluorescence correlation spectroscopy in zero-mode waveguides," Biophys. J. **88**, 2145–2153 (2005).
15. J. B. Edel, M. Wu, B. Baird, and H. G. Craighead, "High spatial resolution observation of single molecule dynamics in living cell membranes," Biophys. J. **88**, L43–L45 (2005).
16. J. Wenger, H. Rigneault, J. Dintinger, D. Marguet, and P. F. Lenne, "Single-fluorophore diffusion in a lipid membrane over a subwavelength aperture," J. Biol. Phys. **32**, SN1–SN4 (2006).
17. Y. Liu and S. Blair, "Fluorescence enhancement from an array of subwavelength metal apertures," Opt. Lett. **28**, 507–509 (2003).
18. Y. Liu, J. Bishop, L. Williams, S. Blair, and J. Herron,

"Biosensing based upon molecular confinement in metallic nanocavity arrays," Nanotechnology **15**, 1368–1374 (2004).
19. Y. Liu, F. Mahdavi, and S. Blair, "Enhanced fluorescence transduction properties of metallic nanocavity arrays," IEEE J. Sel. Top. Quantum Electron. **11**, 778–784 (2005).
20. A. G. Brolo, S. C. Kwok, M. G. Moffitt, R. Gordon, J. Riordon, and K. L. Kavanagh, "Enhanced fluorescence from arrays of nanoholes in a gold film," J. Am. Chem. Soc. **127**, 14936–14941 (2005).
21. J. Wenger, P. F. Lenne, E. Popov, and H. Rigneault, "Single molecule fluorescence in rectangular nano-apertures," Opt. Express **13**, 7035–7044 (2005).
22. N. Bonod, E. Popov, and M. Nevière, "Differential theory of diffraction by finite cylindrical objects," J. Opt. Soc. Am. A **22**, 481–490 (2005).
23. R. Rigler, U. Mets, J. Windengren, and P. Kask, "Fluorescence correlation spectroscopy with high count rate and low-background—analysis of translational diffusion," Eur. Biophys. J. **22**, 169–175 (1993).
24. E. Popov, M. Nevière, A.-L. Fehrembach, and N. Bonod, "Optimization of plasmon excitation at structured apertures," Appl. Opt. **44**, 6141–6154 (2005).
25. A. Snyder and J. Love, *Optical Waveguide Theory* (Chapman & Hall, 1983).
26. S. Enoch, B. Gralak, and G. Tayeb, "Enhanced emission with angular confinement from photonic crystals," Appl. Phys. Lett. **81**, 1588–1590 (2002).
27. F. J. Garcia-Vidal, E. Moreno, J. A. Porto, and L. Martin-Moreno, "Transmission of light through a single rectangular hole," Phys. Rev. Lett. **95**, 103901-1–103901-4 (2005).
28. J. D. Jackson, *Classical Electrodynamics*, 3rd ed. (Wiley, 1998), p. 366.
29. R. W. Wood, "On a remarkable case of uneven distribution of light in a diffraction grating spectrum," Philos. Mag. **4**, 396–402 (1902).
30. R. Petit, ed., *Electromagnetic Theory of Gratings* (Springer, 1980), Chap. 5.
31. D. Maystre, "General study of grating anomalies from electromagnetic surface modes," in *Electromagnetic Surface Modes*, A. D. Boardman, ed. (Wiley, 1982), Chap. 17.
32. E. Popov, "Light diffraction by relief gratings: macro and microscopic point of view," in *Progress in Optics, Vol. XXXII* P. Wolf, ed. (Elsevier, 1993), Chap. 2.
33. M. C. Hutley and D. Maystre, "The total absorption of light by a diffraction grating," Opt. Commun. **19**, 431–436 (1976).
34. E. Popov and L. Tsonev, "Total absorption of light by metallic gratings and energy flow distribution," Surf. Sci. **230**, 290–294 (1990).